

See discussions, stats, and author profiles for this publication at: <https://www.researchgate.net/publication/269574736>

Selective Production of Propylene from Methanol Conversion over Nanosized ZSM-22 Zeolites

ARTICLE *in* INDUSTRIAL & ENGINEERING CHEMISTRY RESEARCH · NOVEMBER 2014

Impact Factor: 2.59 · DOI: 10.1021/ie5038006

CITATIONS

4

READS

37

6 AUTHORS, INCLUDING:



Anas Jamil

King Fahd University of Petroleum and Minerals

4 PUBLICATIONS 8 CITATIONS

[SEE PROFILE](#)



Oki Muraza

King Fahd University of Petroleum and Minerals

59 PUBLICATIONS 171 CITATIONS

[SEE PROFILE](#)



Zain Hasan Yamani

King Fahd University of Petroleum and Minerals

107 PUBLICATIONS 1,569 CITATIONS

[SEE PROFILE](#)



Toshiyuki Yokoi

Tokyo Institute of Technology

128 PUBLICATIONS 3,473 CITATIONS

[SEE PROFILE](#)

Selective Production of Propylene from Methanol Conversion over Nanosized ZSM-22 Zeolites

Anas K. Jamil,[†] Oki Muraza,^{*,†} Masato Yoshioka,[‡] Adnan M. Al-Amer,[†] Zain H. Yamani,[†] and Toshiyuki Yokoi[‡]

[†]Center of Excellence in Nanotechnology and Chemical Engineering Department, King Fahd University of Petroleum and Minerals, Dhahran 31261, Saudi Arabia

[‡]Chemical Resources Laboratory, Tokyo Institute of Technology, 4259 Nagatsuta, Midori-ku, Yokohama, 226-8503, Japan

ABSTRACT: One dimensional pore zeolites such as ZSM-22 (TON) are potential catalysts for hydrocarbon conversion reactions, including methanol-to-propylene (MTP) reaction. Different crystal lengths of ZSM-22 zeolite were prepared and examined for the MTP reaction. Nanosized TON zeolites with crystal length of ~100 nm were synthesized by dynamic hydrothermal synthesis. The zeolite crystal length was tuned by using ethylene glycol as crystal growth modifier. The crystal lengths of ZSM-22 zeolites (approximately 100 and 300 nm) were confirmed from FE-SEM and TEM micrographs. However, the textural properties such as BET surface area and crystallinity of crystals were fairly similar. The effect of ZSM-22 crystal length on catalytic activity and propylene yields in the methanol-to-propylene reaction was investigated. The TON nanocrystals resulted in a higher propylene yield and better catalytic stability compared to the submicrometer zeolite (~300 nm). Deactivation was observed for all catalysts. However, longer lifetime was observed for the nanosized ZSM-22 with crystal length of ~100 nm.

1. INTRODUCTION

Demand for light olefins (ethylene, propylene, and butylene) is growing rapidly every year.^{1–3} The amounts of light olefins, especially the propylene, produced by the conventional methods such as fluid catalytic cracking units (FCC) are not enough to meet the rising demands for propylene.^{1,2} Conversion of alcohols such as methanol^{4,5} and ethanol^{6,7} to light olefins is garnering more attention as a promising alternative to increase propylene production.

Light olefins are intermediate products in the methanol conversion to olefins. To get higher yields of light olefins from this reaction, it is important to prevent the side reactions, where the olefins are consumed and converted to other undesired byproducts. Light olefins have smaller molecular lengths than gasoline-range hydrocarbons molecules. The catalytic conversion of methanol as well as light olefins production occurs basically inside zeolite pores. Therefore, the catalytic activity and light olefins yields are adversely affected by the diffusion resistances of the both the reactant methanol and the produced light olefins. One of the primary strategies to overcome the diffusion resistance within the microspore is by using nanosized zeolites.^{8,9} Faster mass transfer rate can be achieved by decreasing zeolite crystal length, which accordingly decreases the diffusion length of hydrocarbons within zeolite pore.¹⁰

ZSM-22 (TON) zeolite has been reported in the conversion of methanol to olefins (MTO),^{11–20} mainly exploring the viability of ZSM-22 as MTO catalyst. Cui and co-workers^{11–13} reported that ZSM-22 was an inefficient catalyst for the methanol to olefin reaction. The confined space inside pores of ZSM-22 crystals was believed to be insufficient for relatively large molecules involved in hydrocarbon pool mechanism.^{11,16} However, other groups^{14,17,19,21} reported that under suitable conditions, ZSM-22 can produce light olefins via olefin methylation–cracking mechanism (Dassau's mechanism) with

comparable reaction rates to the other commercial zeolites.^{15,17} The one-dimensional pore system and the pore opening size contributed to the high propylene/ethylene (P/E) ratio obtained over ZSM-22.⁴

The effect of zeolite crystal size on the conversion of methanol has been reported recently for SAPO-34^{22–24} and ZSM-5.^{25,26} To the best of our knowledge, there is no report yet regarding the effect of ZSM-22 crystal length on the MTO reaction.

ZSM-22 is a medium-pore zeolite with TON framework that consists of 5, 6, and 10 rings. The TON framework family includes ZSM-22, Theta-1, Nu-10, KZ-2, and ISI-1.^{27–29} The pore structure of ZSM-22 is linear one-dimensional (non-interconnecting) with 10-membered ring openings with effective pore size of 0.45 nm × 0.55 nm, which is smaller than the pore size of ZSM-11 and ZSM-5.^{30–32} This work was devoted to study the effect of ZSM-22 crystal length on the ZSM-22 catalytic and yield of light olefins.

2. EXPERIMENTAL SECTION

2.1. Preparation of ZSM-22 Zeolites with Different Crystal Lengths. Aluminate solution was prepared by adding 0.9 g of aluminum sulfate octadecahydrate and 4.2 g of 1,6-diaminohexane (DAH) to 1.9 g of KOH and 44.2 g of deionized (DI) water. Silicate solution was prepared by adding 18 g of colloidal silica solution to 31 g of DI water. The gel solution was formed by adding silicate solution to aluminate solution. The initial molar composition of the prepared gel was 1 Al₂O₃/91.4 SiO₂/26.5 K₂O/27.4 DAH/3202 H₂O. Ethylene

Received: September 25, 2014

Revised: November 19, 2014

Accepted: November 25, 2014

Published: November 25, 2014

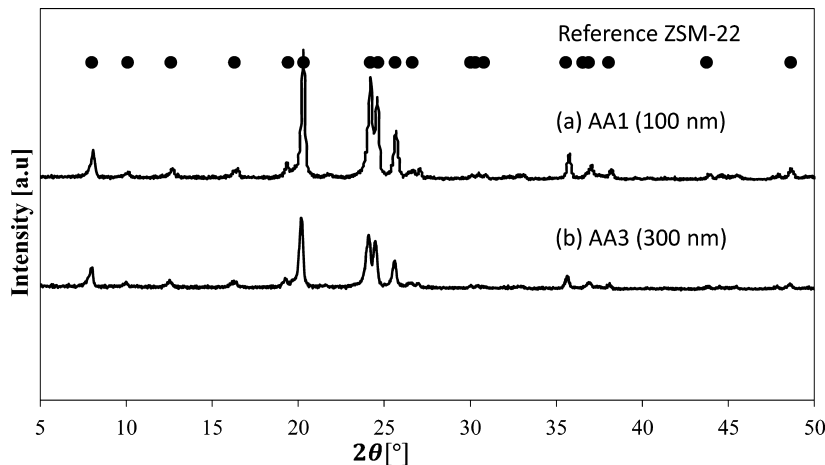


Figure 1. X-ray diffraction patterns of ZSM-22 zeolite with different crystal sizes: (a) AA1 (100 nm); (b) AA3 (300 nm).

glycol as a cosolvent was added to the synthesis gel. The gel was aged at 50 °C for 2 h, and subsequently the crystallization was performed in a rotating autoclave at 180 °C and rotation 67 rpm for 36 h.

The resulting powder was centrifuged and dried for 12 h at 120 °C. The sample then was calcined at 550 °C for 8 h under a flow of air with heating rate of 1 °C/min.

The calcined zeolites (K-ZSM-22) were transformed to NH₄-ZSM-22 by ion exchange with 2 M ammonium nitrate (NH₄NO₃) under microwave irradiation.³³ K-ZSM-22 zeolite sample (2 g) was mixed with 20 mL of NH₄NO₃ solution (2 M) where the ratio of NH₄NO₃ solution volume to zeolite weight ratio was 20. The temperature was ramped from room temperature to 85 °C in 5 min using 800 W irradiation power. Then ion-exchange step was performed at 85 °C for 10 min (400 W irradiation power). The mixture was cooled and centrifuged to separate ZSM-22 zeolite from the mixture. The whole process was repeated again to ensure complete ion exchange from K-ZSM-22 to NH₄-ZSM-22. The NH₄-ZSM-22 was then calcined again to obtain H-ZSM-22. The H-ZSM-22 zeolite was pelletized and sieved in the range of 300–500 μm.

2.2. Characterization of ZSM-22 Zeolite. ZSM-22 catalysts were characterized using powder X-ray diffraction (XRD), scanning electron microscopy (SEM), N₂ adsorption–desorption measurements (BET measurement), infrared spectroscopy (FTIR), transmission electron microscope (TEM), temperature-programmed desorption (TPD), and thermogravimetry (TG). Finally, the catalytic behavior of the resulted ZSM-22 crystals was investigated in a catalytic packed bed reactor.

Crystalline phases of synthesized crystals were identified using Rigaku X-ray diffractometer with a step size of 0.03°, with Bragg–Brentano geometry, position sensitive detector, and Cu K α radiation ($\lambda = 1.5406 \text{ \AA}$). XRD data were analyzed using EVA 8.0 (Rigaku).

The crystal length and morphology were investigated using scanning electron microscopy. ZSM-22 crystals were spread on a sample holder using a volatile solvent (ethanol). Low acceleration voltage (15 kV) and spot size 3 were used for imaging. The equipment used was SEM-FIB Tescan Lyra. The ZSM-22 catalyst was suspended in ethanol, and a drop of the mixture was spread and dried on porous carbon film sample cell. We analyzed the dried specimens using electron microscope. The specific surface area of ZSM-22 catalysts was

determined by nitrogen adsorption at a temperature of 77 K. An amount of about 60 mg of the catalysts was pretreated for 5 h prior to the surface area measurements. The pretreatment was carried out by outgassing the catalysts at 80 °C for 1 h followed by 4 h at 300 °C. FT-IR spectra were recorded on FT-IR (JASCO FT-IR 4100) with MCT detector, 4 cm⁻¹ resolution, and 64 numbers of scan. The surface of ZSM-22 zeolite sample was pretreated at a temperature 773 K under evacuation for 1 h. The sample was cooled to 423 K, and pyridine was used as probe molecule and loaded at 423 K. The evacuation was done at 523 K, and the IR spectra of the pyridine with the ZSM-22 zeolite samples were measured and recorded at 423 K. The acid strength distribution of the ZSM-22 zeolite crystals was investigated using ammonia temperature-programmed desorption (NH₃-TPD). For each experiment, 150 mg of the catalyst sample was degassed using helium gas (30 mL/min) for 2 h at 300 °C. Then the sample was cooled to 100 °C and saturated with ammonia gas, which was then removed gradually by using helium gas. Temperature was then raised to 500 °C. In the meantime, the adsorbed ammonia was starting to desorb. Different heating rates (10, 15, and 20 °C/min) were used to desorb ammonia from the catalyst sample. The NH₃-TPD experiments were carried out using AutoChem II analyzer from Micrometrics. Coke amount was analyzed by measuring weight loss of the sample using thermogravimetry (TG) in a temperature range from 673 to 1073 K.

2.3. Evaluation of Catalyst Activity. The catalytic behavior of the resulting ZSM-22 crystals was evaluated for the conversion of methanol to light olefins in a catalytic packed bed reactor. The catalytic conversion of methanol was carried out over H-ZSM-22 catalysts in a packed bed reactor. The catalyst weight was 100 mg pelletized and sieved in the range of 300–500 μm. Methanol was diluted in helium (He) gas. To study the influence of reaction parameters, methanol concentration was varied from 2.5% to 5% and W/F between 33 and 67 g·h·mol⁻¹. The reaction temperature was varied between 350 and 500 °C. However, most of the experiments were performed at 2.5% methanol concentration, W/F = 67 g·h·mol⁻¹ and temperature of 450 °C. The reaction products were analyzed by online gas chromatographs (GC, Shimadzu GC-2014) (GC-14B, Shimadzu Corporation) and a CG–MS (Agilent Technologies, GC-7890Q and MS-5975C with triple-axis detector) instrument with a HP plot column, and more details about the methanol reaction experiments were described

by Zhu and co-workers.³⁴ Terms of methanol conversion, product selectivity, and yield are defined and calculated by the following eqs 1, 2, and 3:

$$\text{MeOH conversion (\%)} = \frac{(\text{moles of MeOH fed}) - (\text{moles of MeOH unreacted})}{(\text{moles of MeOH fed})} \times 100 \quad (1)$$

$$\text{product carbon selectivity (\%)} = \frac{(\text{moles of carbon atom in specific product produced})}{(\text{moles of MeOH fed}) - (\text{moles of MeOH unreacted})} \times 100 \quad (2)$$

$$\text{product carbon yield (\%)} = \frac{(\text{moles of carbon atom in specific product produced})}{(\text{moles of MeOH fed})} \times 100 \quad (3)$$

3. RESULTS AND DISCUSSIONS

3.1. Characteristics of ZSM-22 Zeolite Samples. Pure ZSM-22 zeolites with two different crystal lengths were prepared by different methods. Nanosized ZSM-22 with crystal length of ~100 nm (code AA1) was synthesized via hydrothermal autoclave with horizontal rotation of 67 rpm. The submicrometer ZSM-22 (300 nm, sample code AA3) was obtained by adding 5 wt % of ethylene glycol to the synthesis mixture. The purity of ZSM-22 phase was confirmed by analyzing the XRD patterns of the two samples (see Figure 1), and as expected, the peaks patterns for the two samples are identical with standard peaks for ZSM-22. The Si/Al ratios for the prepared samples were measured using XRF analysis, and they were almost similar to the initial gel Si/Al ratios (see Table 1). Figure 2 shows that the morphology for the samples was

Table 1. Physicochemical Properties of ZSM-22 Zeolite with Different Crystal Sizes^a

| sample | size ^b [nm] | Si/Al ratio ^c | Si/Al ratio ^d | S_{BET} [$\text{m}^2 \text{g}^{-1}$] | S_{ext} [$\text{m}^2 \text{g}^{-1}$] | V_{micro} [$\text{cm}^3 \text{g}^{-1}$] |
|--------|------------------------|--------------------------|--------------------------|---|---|--|
| AA1 | 100 | 46 | 44.0 | 201 | 48 | 0.06 |
| AA3 | 300 | 46 | 43.7 | 201 | 41 | 0.06 |

^a S_{BET} : surface area by BET method. S_{ext} : external surface area by t-method. V_{micro} : micropore volume by t-method. ^b Crystal size approximated using SEM images. ^c Calculated in the synthesis gel. ^d Analyzed using XRF.

rod shaped crystals with average crystal lengths of approximately 100 and 300 nm for samples AA1 and AA3, respectively. The physicochemical properties of ZSM-22 zeolite samples are summarized in Table 1.

Further investigation of size and morphology was carried out for sample AA1 by using TEM images (Figure 3). As expected, the nanosized sample observed using SEM (Figure 2a) was confirmed with TEM micrographs. Figure 4 shows the NH₃-TPD profiles of nanosized and submicrometer ZSM-22 crystals. Both samples have a strong peak around 460 K (187 °C), which corresponds to weak acid sites. However, the submicrometer ZSM-22 crystals have negligible strong acid sites, which appear around 670 K (397 °C) for AA1. The

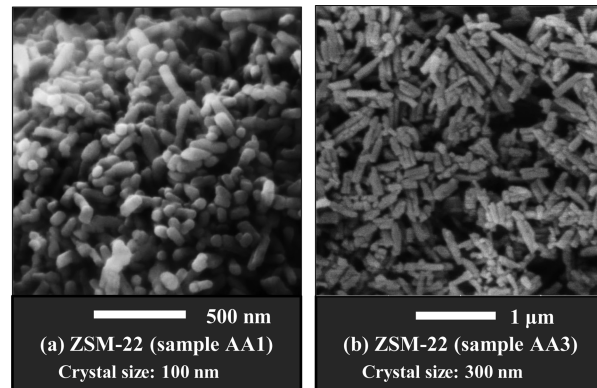


Figure 2. SEM images of ZSM-22 zeolite with different crystal sizes: (a) AA1 (100 nm); (b) AA3 (300 nm).

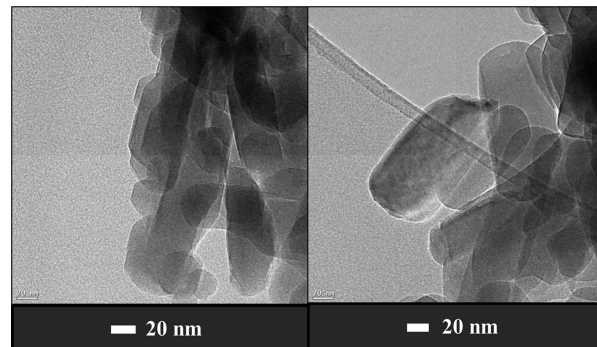


Figure 3. TEM images of nanosized ZSM-22 crystal, sample AA1 (100 nm).

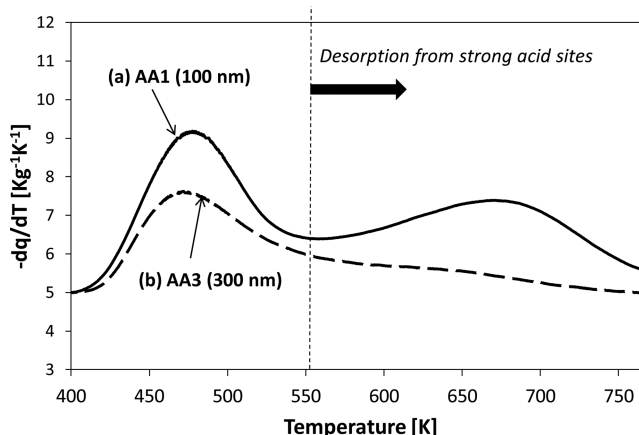


Figure 4. NH₃-temperature-programmed desorption profiles of H-ZSM-22 zeolites with different crystal sizes: (a) AA1(100 nm); (b) AA3 (300 nm).

pyridine FT-IR analysis of both ZSM-22 zeolite samples confirms that the nanosized AA1 has slightly higher Lewis acidity (Figures 4 and 5 and Table 2).

The nanosized ZSM-22 crystals have slightly larger external surface area than the submicrometer ZSM-22 crystals (AA3). The surface area of the prepared samples was measured using the N₂ adsorption-desorption measurements (BET measurement) (see Figure 6 and Table 1). As shown in Table 1, the BET surface areas were almost similar ($201 \text{ m}^2 \text{ g}^{-1}$) for both samples AA1 and AA3, while the smaller crystal size (AA1) has a larger external surface than AA3. The external surface areas

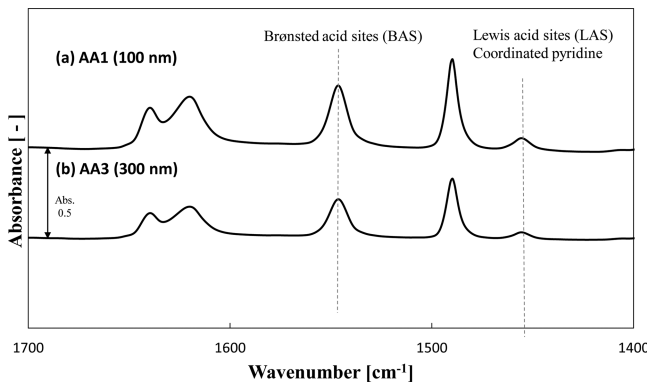


Figure 5. Pyridine FTIR analysis of ZSM-22 zeolite with different crystal sizes: (a) AA1 (100 nm); (b) AA3 (300 nm).

Table 2. Acid Properties of ZSM-22 Zeolite Samples

| sample | FTIR area _{BAS} /area _{LAS} ^a | ammonia TPD (mmol NH ₃ /g solid) | | | |
|-----------------|---|---|-------------------|---------------------|-------------|
| | | total | weak ^b | strong ^c | strong/weak |
| AA1 (100 nm) | 6.2 | 1.25 | 0.53 | 0.72 | 1.35 |
| AA3 (300 nm) | 7.4 | 0.97 | 0.50 | 0.47 | 0.95 |

^aBronsted/Lewis acid sites ratio was calculated by measuring the peaks at 1540 and 1450 cm^{-1} . Pyridine desorption temperature, 150 °C.

^bThe density of weak acid sites was calculated by measuring the area under peaks between temperatures 370 and 500 K. ^cThe density of strong acid sites was calculated by measuring the area under peaks between temperatures 500 and 815 K.

were 48 and 41 $\text{m}^2 \cdot \text{g}^{-1}$ for the nanosized crystals (AA1) and submicrometer crystals (AA3), respectively. Meanwhile, the crystal micropore volumes remained unchanged. Similar results were reported in the literature for ZSM-5 zeolite.¹

3.2. Methanol Conversion to Light Olefins over H-ZSM-22 Zeolite Crystals. The effect of temperature on the ZSM-22 catalytic activity was first investigated. Figure 7 shows the effect of reaction temperature on the methanol conversion and the product selectivity at a WHSV of 0.972 $\text{g} \cdot \text{g}^{-1} \cdot \text{h}^{-1}$. Reaction products were classified into four groups. The first group contained light olefins, which include ethylene, propylene, and butylene. The second group contained paraffins, which consist of methane, ethane, propane, and butanes. The last groups contained heavier olefins and, starting from pentene and higher, paraffins (C_5 and above) and aromatics such as benzene, toluene, and xylene (BTX).

As can be seen in Figure 7, the reaction at low temperature (350 °C) resulted in lower conversion of 86% as diffusion of methanol and product molecules within ZSM-22 crystals was obstructed.³⁵ High temperature (450 °C) stimulates pressure difference across the pore, ensuring satisfying mass flow,³⁵ and therefore, complete conversion of methanol combined with high light olefins selectivity (73%) and excellent propylene yield (42%) was achieved.

Methanol conversion and yield of light olefins, especially for propylene, were increased by increasing temperature. Dimethyl ether (DME) was the major product at low temperature (350 °C). However, it was completely converted to olefins at higher temperatures (400–450 °C). The temperature over 400 °C is essential for the conversion of DME to olefins (further dehydration reaction).^{36,37} Below 300 °C, there was no dehydration of DME. As shown in Figure 8a, the WHSV (weight hourly space velocity) affected the catalyst life severely.

The selectivity to light olefins and over C_5 hydrocarbons increased noticeably with increasing temperature from 350 to 400 °C. Further increase in temperature from 400 to 450 °C dehydrated the heavier hydrocarbons to produce more light olefins,³⁸ specifically propylene and butylene. The selectivity to heavier hydrocarbon (over C_5) decreased from 36% to 24%, while light olefins selectivity increased from 56 to 72%.

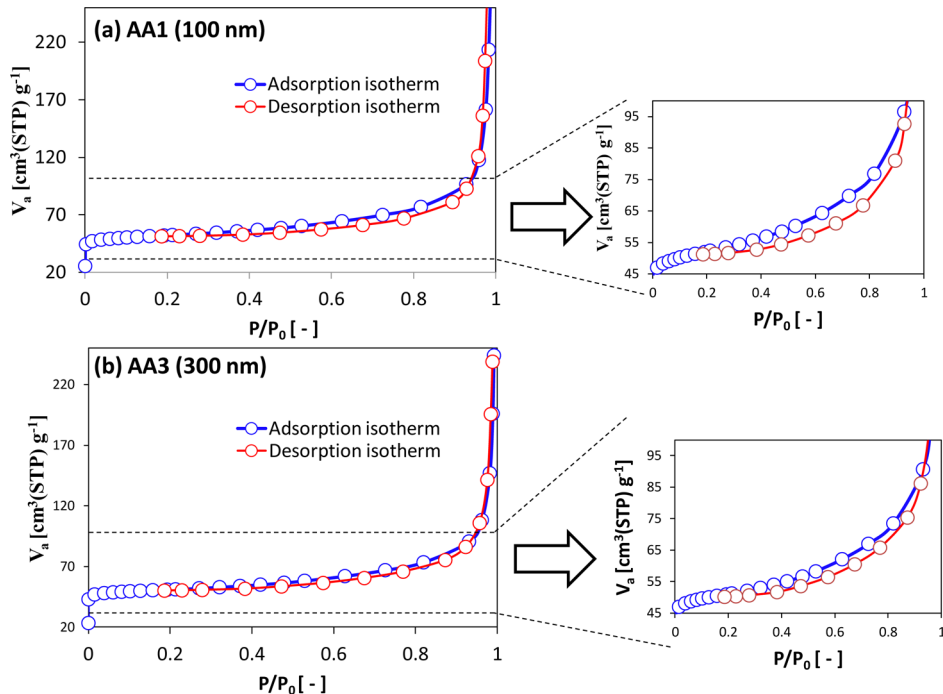
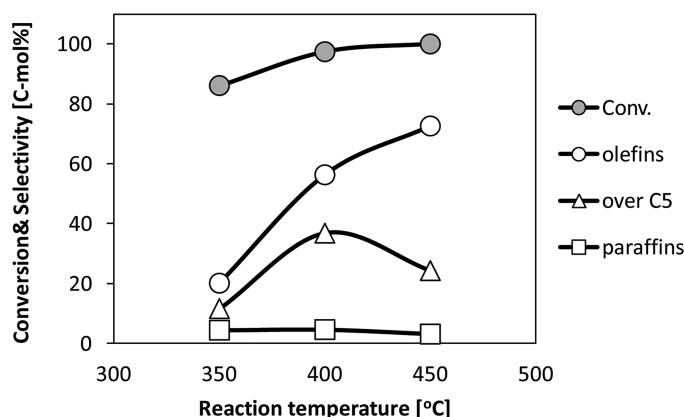


Figure 6. N_2 adsorption–desorption isotherm (BET) of ZSM-22 zeolite with different crystal sizes: (a) AA1 (100 nm); (b) AA3 (300 nm).

(a) Methanol conversion and products selectivity.



(b) Olefins yield

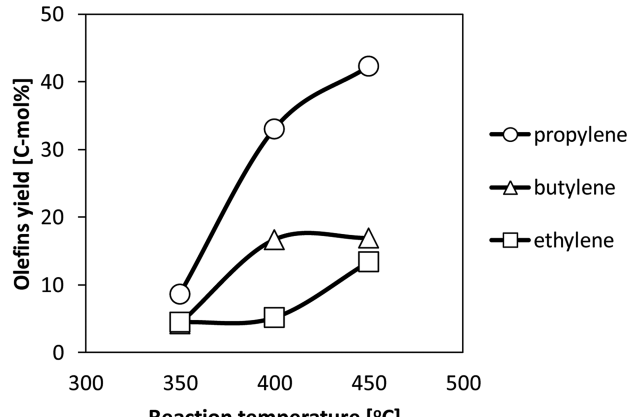
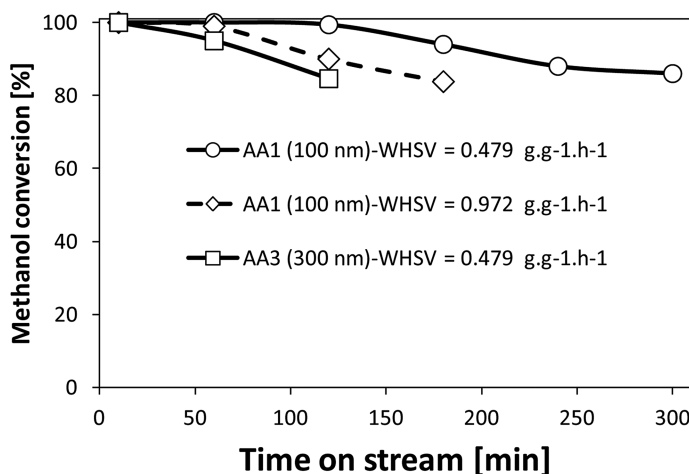


Figure 7. Effect of temperature on (a) methanol conversion and product selectivity and (b) olefins yield. Reaction was carried out over sample AA1 (100 nm), WHSV = 0.972 g·g⁻¹·h⁻¹.

(a) Conversion of the methanol



(b) amount of coke after 180 min

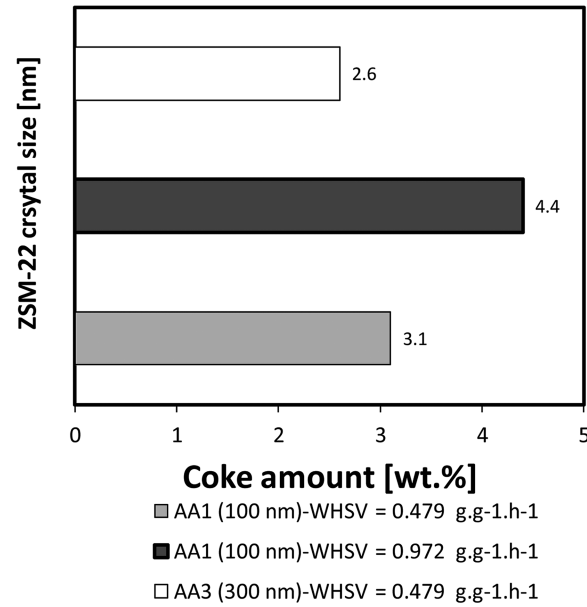


Figure 8. Effect of crystal size on (a) conversion of the methanol and (b) amount of coke after 180 min. Reaction was carried out over H-ZSM-22 at 450 °C.

Decreasing WHSV obviously increased catalytic stability of sample (AA1) and decreased the amount of the coke deposited on sample (AA1). From Figure 8b, the amount of coke deposited after 180 min of reaction over sample AA1 (100 nm) was 3.1%, and for sample AA3 (300 nm) it was 2.6%. The catalytic stability decay with time on stream is affected by methanol flow. In general, at high methanol flow (WHSV = 0.972 g·g⁻¹·h⁻¹), successive reactions of the products easily occurred, resulting in the coke formation as clearly observed from Figure 8b. At the same WHSV (WHSV = 0.497 g·g⁻¹·h⁻¹), the amount of coke deposited over ZSM-22 crystals increased with decreasing crystal length, since the smaller crystal sample AA1 (100 nm) has higher external area and more pore mouths.

3.3. Effect of ZSM-22 Crystal Length on Methanol to Olefins Reaction.

The effects of zeolite crystal length on

methanol conversion, product selectivity, and light olefins yield with the change of time on stream are presented in Figure 9 and Table 3. The reactions were run at 450 °C and WHSV = 0.479 g·g⁻¹·h⁻¹. Larger ZSM-22 zeolite crystals (AA3) deactivated faster by the pore blocking than the smaller ZSM-22 crystals (AA1) as indication of the slower deactivation rate over the smaller crystals (see Figure 9). Regardless of the ZSM-22 crystal length, methanol conversion declined with time because of coke formation on the acid sites located on pore mouths and external surfaces of ZSM-22 crystals.^{14,20} Since sample AA1 has higher external surface area ($48 \text{ m}^2 \cdot \text{g}^{-1}$), larger number of pore mouths, and shorter crystal length than sample AA3 (300 nm) with external surface area of $41 \text{ m}^2 \cdot \text{g}^{-1}$ (see Table 1), more coke is required to deactivate the external surface area and pore mouths of sample AA1. Hence AA1 sample exhibited higher catalytic activity as compared with the

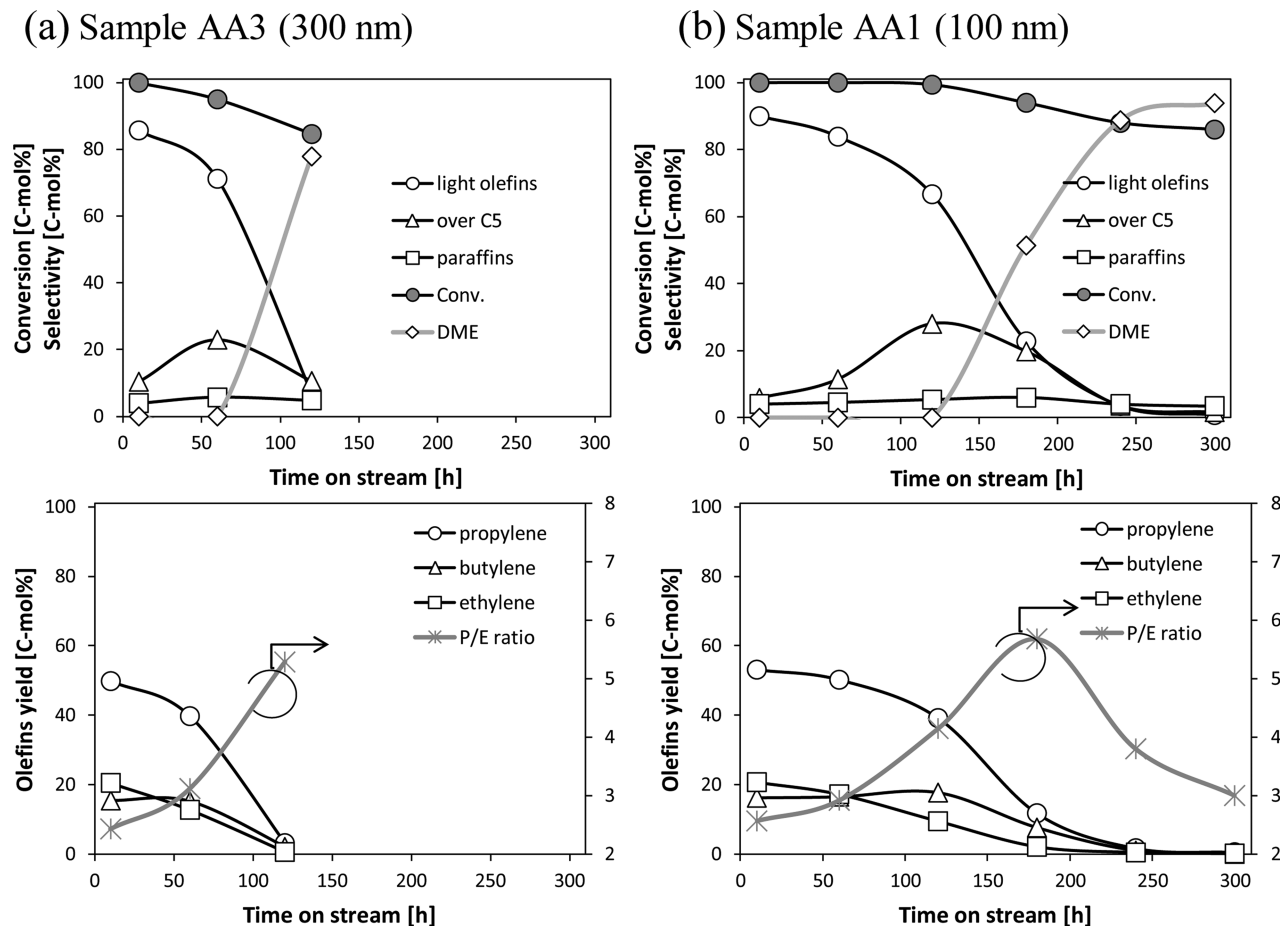


Figure 9. Methanol conversion and product selectivity, light olefin yields, and propylene/ethylene ratio (*P/E* ratio) vs reaction time at 450 °C and WHSV = 0.479 g·g⁻¹·h⁻¹ over the H-ZSM-22 different crystal sizes: (a) AA67 (100 nm); (b) AA3 (300 nm).

Table 3. Methanol Conversions and Product Yields over H-ZSM-22 Zeolite (Si/Al = 46) with Different Crystal Sizes^a

| time [min] | conversion [%] | light olefins yield [C-mol %] | | | | | over C ₅ yield [C-mol %] | paraffins yield [C-mol %] | <i>P/E</i> ratio |
|-----------------------|----------------|-------------------------------|----------------|----------------|---------------|--|-------------------------------------|---------------------------|------------------|
| | | C ₂ | C ₃ | C ₄ | total olefins | | | | |
| Sample = AA1 (100 nm) | | | | | | | | | |
| 10 | 100 | 21 | 53 | 16 | 90 | | 6 | 4.1 | 2.6 |
| 120 | 99.4 | 9 | 40 | 18 | 66 | | 28 | 5.4 | 4.1 |
| 240 | 88 | 0.4 | 2 | 1 | 3 | | 3 | 3.6 | 3.8 |
| Sample = AA3 (300 nm) | | | | | | | | | |
| 10 | 100 | 21 | 50 | 15 | 86 | | 10 | 4 | 2.4 |
| 60 | 95 | 13 | 40 | 15 | 68 | | 22 | 5.4 | 3.1 |
| 120 | 84.6 | 0.6 | 3 | 2 | 6 | | 9 | 4 | 5 |

^aReaction conditions: $T = 723\text{ K}$ (450 °C), WHSV = 2.03 g·g⁻¹·h⁻¹.

larger size sample AA3 as shown in Figure 9. On the other hand, the smaller external surface area of sample AA3 made it easier to be poisoned by coke species.

Regardless of the crystal length of ZSM-22 samples, the initial conversion of methanol was almost the same (approximately 100%). As presented in Figure 9 and Table 3, the conversion over sample AA1 was steady at 100% until 120 min. Then conversion decreased gradually over time to 86% after 300 min, while a rapid decline in sample AA3 activity was noticed to 84% conversion after 120 min. Initially, high selectivity of olefins was obtained over ZSM-22 zeolites. However, the selectivity for olefins decreased with time on stream. This decreasing trend is probably because of the increase in the formation of C₅ hydrocarbons (aromatics and

heavier olefins) via the methylation of the formed light olefins. Because of spatial restrictions within tubular pores (0.55 nm × 0.45 nm) of ZSM-22 crystals, methanol converted selectively over the acid sites on the internal surfaces of the pore into light olefins via olefin methylation-cracking mechanism (Dassau's mechanism).^{15,17} Unfortunately, the produced light olefins can be easily consumed into higher olefins, paraffins, and aromatics via a series of methylation reactions over ZSM-22 crystal pore mouths and external surfaces via the dual-cycle mechanism.³⁹

The yield of light olefins can be enhanced by preventing the side reactions; for instance, the reactant (methanol) can be converted over the external surface of the crystals via hydrocarbon pool cycle mechanism. In addition, the products (olefins) may further react with the catalysts, be it through

hydrocarbon pool mechanism or olefin methylation-cracking mechanism.¹⁹

The effect of crystal length on the product distribution can be seen in Table 3. Noticeably, propylene yields over nanocrystal sample (AA1) were 53%, 40%, and 2% after time-on-stream of 10, 120, and 240 min, respectively, while for sample AA3, propylene yields were 50%, 40%, and 3% over time on stream 10, 60, and 120 min, respectively. Change in the yields of propylene, C₅ hydrocarbons, and paraffins with methanol conversion over samples AA1 and AA3 is presented in Table 3. Initially, at 100% conversion of methanol, propylene yield was slightly higher over sample AA1 (53%) than sample AA3 (50%).

4. CONCLUSIONS

Production of light olefins from methanol conversion was examined over ZSM-22 (TON) zeolites with different crystal lengths (100 and 300 nm). Pure nanosized ZSM-22 crystals (100 nm) were synthesized with low aspect ratio by using a hydrothermal autoclave with horizontal rotation, while the submicrometer ZSM-22 crystals (~300 nm) were achieved by using 5 wt % ethylene glycol as a crystal growth modifier. The textural properties were almost similar for both samples with different crystal sizes, except the smaller crystals had larger external surface area. High selectivity to light olefins (>86%) combined with low selectivity toward the undesired over C₅ hydrocarbons (10%) and paraffins (4%) was observed initially over all ZSM-22 zeolite samples. As compared with the submicrometer crystals (300 nm), the 100 nm crystals showed better catalytic activity. The higher catalytic activity of TON nanocrystals can be attributed to the higher external surface area. Therefore, the diffusion problem caused by pore blocking was noticeably reduced.

■ AUTHOR INFORMATION

Corresponding Author

*O.M.: e-mail, omuraza@kfupm.edu.sa.

Notes

The authors declare no competing financial interest.

■ ACKNOWLEDGMENTS

The authors thank Jerwin C. Separa and Dr. Abbas Hakeem for part of the FE-SEM experiments. The authors acknowledge the funding provided by King Abdulaziz City for Science and Technology (KACST) through the Science and Technology Unit in Center of Research Excellence in Nanotechnology at King Fahd University of Petroleum and Minerals (KFUPM) for supporting this work through Project No. 11-NAN2166-04 as part of the National Science, Technology and Innovation Plan.

■ REFERENCES

- Jiao, Y. Supply & Demand Status of Propylene Market and Its Development Trends. *Petrochem. Ind. Trends* **2004**, *9*, 009.
- James, R.; Vermeiren, W. Options for Meeting the Propylene Supply-Demand Gap. Presented at the AIChE Spring National Meeting, New Orleans, LA, 2004.
- Koempel, H.; Liebner, W. Lurgi's Methanol to Propylene (MTP) Report on a Successful Commercialisation. *Stud. Surf. Sci. Catal.* **2007**, *167*, 261–267.
- Stöcker, M. Methanol-to-Hydrocarbons: Catalytic Materials and Their Behavior. *Microporous Mesoporous Mater.* **1999**, *29*, 3–48.

- Keil, F. J.; Hinderer, J.; Garayhi, A. R. Diffusion and Reaction in ZSM-5 and Composite Catalysts for the Methanol-to-Olefins Process. *Catal. Today* **1999**, *50*, 637–650.
- Dao, L. H.; Le Van Mao, R. Ethylene Light Olefins from Ethanol. US4698452 A, 1987.
- Schulz, J.; Bandermann, F. Conversion of Ethanol over Zeolite H-ZSM-5. *Chem. Eng. Technol.* **1994**, *17*, 179–186.
- Tosheva, L.; Valtchev, V. P. Nanozeolites: Synthesis, Crystallization Mechanism, and Applications. *Chem. Mater.* **2005**, *17*, 2494–2513.
- Larsen, S. C. Nanocrystalline Zeolites and Zeolite Structures: Synthesis, Characterization, and Applications. *J. Phys. Chem. C* **2007**, *111*, 18464–18474.
- Grinberg, F.; Heitjans, P. *Diffusion Fundamentals Leipzig* 2005; Leipziger Universitätsverlag: Leipzig, Germany, 2005; Vol. 1.
- Cui, Z. M.; Liu, Q.; Song, W. G.; Wan, L. J. Insights into the Mechanism of Methanol-to-Olefin Conversion at Zeolites with Systematically Selected Framework Structures. *Angew. Chem., Int. Ed.* **2006**, *45*, 6512–6515.
- Cui, Z.-M.; Liu, Q.; Bain, S.-W.; Ma, Z.; Song, W.-G. The Role of Methoxy Groups in Methanol to Olefin Conversion. *J. Phys. Chem. C* **2008**, *112*, 2685–2688.
- Cui, Z.-M.; Liu, Q.; Ma, Z.; Bian, S.-W.; Song, W.-G. Direct Observation of Olefin Homologations on Zeolite ZSM-22 and Its Implications to Methanol to Olefin Conversion. *J. Catal.* **2008**, *258*, 83–86.
- Li, J.; Wei, Y.; Liu, G.; Qi, Y.; Tian, P.; Li, B.; He, Y.; Liu, Z. Comparative Study of MTO Conversion over SAPO-34, H-ZSM-5 and H-ZSM-22: Correlating Catalytic Performance and Reaction Mechanism to Zeolite Topology. *Catal. Today* **2011**, *171*, 221–228.
- Li, J.; Wei, Y.; Qi, Y.; Tian, P.; Li, B.; He, Y.; Chang, F.; Sun, X.; Liu, Z. Conversion of Methanol over H-ZSM-22: The Reaction Mechanism and Deactivation. *Catal. Today* **2011**, *164*, 288–292.
- Wang, Q.; Cui, Z.-M.; Cao, C.-Y.; Song, W.-G. 0.3 Å Makes the Difference: Dramatic Changes in Methanol-to-Olefin Activities between H-ZSM-12 and H-ZSM-22 Zeolites. *J. Phys. Chem. C* **2011**, *115*, 24987–24992.
- Teketel, S.; Svelle, S.; Lillerud, K. P.; Olsbye, U. Shape-Selective Conversion of Methanol to Hydrocarbons over 10-Ring Unidirectional-Channel Acidic H-ZSM-22. *ChemCatChem* **2009**, *1*, 78–81.
- Teketel, S.; Skistad, W.; Benard, S.; Olsbye, U.; Lillerud, K. P.; Beato, P.; Svelle, S. Shape Selectivity in the Conversion of Methanol to Hydrocarbons: The Catalytic Performance of One-Dimensional 10-Ring Zeolites: ZSM-22, ZSM-23, ZSM-48, and EU-1. *ACS Catal.* **2011**, *2*, 26–37.
- Teketel, S.; Olsbye, U.; Lillerud, K.-P.; Beato, P.; Svelle, S. Selectivity Control through Fundamental Mechanistic Insight in the Conversion of Methanol to Hydrocarbons over Zeolites. *Microporous Mesoporous Mater.* **2010**, *136*, 33–41.
- Wei, F.-F.; Cui, Z.-M.; Meng, X.-J.; Cao, C.-Y.; Xiao, F.-S.; Song, W.-G. Origin of the Low Olefin Production over HZSM-22 and HZSM-23 Zeolites: External Acid Sites and Pore Mouth Catalysis. *ACS Catal.* **2014**, *4*, 529–534.
- Li, J.; Qi, Y.; Liu, Z.; Liu, G.; Zhang, D. Co-Reaction of Ethene and Methylation Agents over SAPO-34 and ZSM-22. *Catal. Lett.* **2008**, *121*, 303–310.
- Hirota, Y.; Murata, K.; Miyamoto, M.; Egashira, Y.; Nishiyama, N. Light Olefins Synthesis from Methanol and Dimethylether over SAPO-34 Nanocrystals. *Catal. Lett.* **2010**, *140*, 22–26.
- Dai, W.; Wu, G.; Li, L.; Guan, N.; Hunger, M. Mechanisms of the Deactivation of SAPO-34 Materials with Different Crystal Sizes Applied as MTO Catalysts. *ACS Catal.* **2013**, *3*, 588–596.
- Chen, D.; Moljord, K.; Fuglerud, T.; Holmen, A. The Effect of Crystal Size of SAPO-34 on the Selectivity and Deactivation of the MTO Reaction. *Microporous Mesoporous Mater.* **1999**, *29*, 191–203.
- Herrmann, C.; Haas, J.; Fetting, F. Effect of the Crystal Size on the Activity of ZSM-5 Catalysts in Various Reactions. *Appl. Catal.* **1987**, *35*, 299–310.

- (26) Firoozi, M.; Baghalha, M.; Asadi, M. The Effect of Micro and Nano Particle Sizes of H-ZSM-5 on the Selectivity of MTP Reaction. *Catal. Commun.* **2009**, *10*, 1582–1585.
- (27) Baerlocher, C.; McCusker, L. B.; Olson, D. H. *Atlas of Zeolite Framework Types*; Elsevier: Amsterdam, 2007.
- (28) Dwyer, F. G.; Valyocsik, E. W. Highly Siliceous Porous Crystalline Material. US5336478 A, 1994.
- (29) Fyfe, C. A.; Kokotailo, G. T.; Strobl, H.; Pasztor, C.; Barlow, G.; Bradley, S. Combined Use of Nuclear Magnetic Resonance, Electron Microscopy, and Diffraction Techniques as a Probe of the Uniqueness of Zeolite Structures: Zeolites KZ-2, Theta-1, ZSM-22, and NU-10. *Zeolites* **1989**, *9*, 531–534.
- (30) Kokotailo, G.; Chu, P.; Lawton, S.; Meier, W. Synthesis and Structure of Synthetic Zeolite ZSM-11. *Nature* **1978**, *275*, 119–120.
- (31) Kokotailo, G.; Schlenker, J.; Dwyer, F.; Valyocsik, E. The Framework Topology of ZSM-22: A High Silica Zeolite. *Zeolites* **1985**, *5*, 349–351.
- (32) Valyocsik, E. W. Synthesis of Zeolite ZSM-22 with a Heterocyclic Organic Compound. US4481177 A, 1984.
- (33) Lopes, J.; Serralha, F.; Costa, C.; Lemos, F.; Ribeiro, F. R. Preparation of HNaY Zeolite by Ion Exchange under Microwave Treatment. A Preliminary Study. *Catal. Lett.* **1998**, *53*, 103–106.
- (34) Zhu, Q.; Kondo, J. N.; Ohnuma, R.; Kubota, Y.; Yamaguchi, M.; Tatsumi, T. The Study of Methanol-to-Olefin over Proton Type Aluminosilicate CHA Zeolites. *Microporous Mesoporous Mater.* **2008**, *112*, 153–161.
- (35) Thomas, J. M.; Thomas, W. J.; Anderson, J.; Boudart, M. *Principles and Practice of Heterogeneous Catalysis*; VCH: Weinheim, Germany, 1997; Vol. 638.
- (36) Froment, G.; Dehertog, W.; Marchi, A. Zeolite Catalysis in the Conversion of Methanol into Olefins. *Catalysis* **1992**, *9*, 1–64.
- (37) Travalloni, L.; Gomes, A. C.; Gaspar, A. B.; da Silva, M. A. Methanol Conversion over Acid Solid Catalysts. *Catal. Today* **2008**, *133*, 406–412.
- (38) Bhasin, M.; McCain, J.; Vora, B.; Imai, T.; Pujado, P. Dehydrogenation and Oxydehydrogenation of Paraffins to Olefins. *Appl. Catal., A* **2001**, *221*, 397–419.
- (39) Svelle, S.; Joensen, F.; Nerlov, J.; Olsbye, U.; Lillerud, K.-P.; Kolboe, S.; Bjørgen, M. Conversion of Methanol into Hydrocarbons over Zeolite H-ZSM-5: Ethene Formation Is Mechanistically Separated from the Formation of Higher Alkenes. *J. Am. Chem. Soc.* **2006**, *128*, 14770–14771.